

PAPER • OPEN ACCESS

## A new kaonic helium measurement in gas by SIDDHARTINO at the DAΦNE collider








To cite this article: D Sirghi *et al* 2022 *J. Phys. G: Nucl. Part. Phys.* **49** 055106

View the [article online](#) for updates and enhancements.

### You may also like

- [Kaonic helium X-ray measurement in the SIDDHARTINO experiment](#)  
H Shi, M Bazzi, G Beer *et al.*
- [The kaonic atoms research program at DANE: overview and perspectives](#)  
C Curceanu, A Amirkhani, A Baniahmad *et al.*
- [Probing low-energy QCD with kaonic atoms at DANE](#)  
M Tüchler, J Zmeskal, A Amirkhani *et al.*

# A new kaonic helium measurement in gas by SIDDHARTINO at the DAΦNE collider\*

D Sirghi<sup>1,2</sup>, F Sirghi<sup>1,2</sup>, F Sgaramella<sup>1,\*\*</sup> , M Bazzi<sup>1</sup>,  
D Bosnar<sup>3</sup> , M Bragadireanu<sup>2</sup>, M Carminati<sup>4</sup>, M Cargnelli<sup>5</sup>,  
A Clozza<sup>1</sup>, G Deda<sup>4</sup>, L De Paolis<sup>1</sup>, R Del Grande<sup>1,6</sup> ,  
L Fabbietti<sup>6</sup>, C Fiorini<sup>4</sup>, C Guaraldo<sup>1</sup>, M Iliescu<sup>1</sup>, M Iwasaki<sup>7</sup>,  
P Levi Sandri<sup>1</sup>, J Marton<sup>5</sup>, M Miliucci<sup>1</sup> , P Moskal<sup>8</sup> ,  
F Napolitano<sup>1</sup> , S Niedźwiecki<sup>8</sup>, K Piscicchia<sup>1,9</sup>,  
A Scordo<sup>1,\*\*</sup> , H Shi<sup>5</sup>, M Skurzok<sup>8</sup>, M Silarski<sup>8</sup>,  
A Spallone<sup>1</sup>, M Tüchler<sup>5</sup>, O Vazquez Doce<sup>1</sup>, J Zmeskal<sup>5</sup>  
and C Curceanu<sup>1</sup>

<sup>1</sup> Laboratori Nazionali di Frascati INFN, Via E. Fermi 54, 00044 Frascati, Italy

<sup>2</sup> Horia Hulubei National Institute of Physics and Nuclear Engineering (IFIN-HH) Măgurele, Romania

<sup>3</sup> Department of Physics, Faculty of Science, University of Zagreb, Zagreb, Croatia

<sup>4</sup> Politecnico di Milano, Dipartimento di Elettronica, Informazione e Bioingegneria and INFN Sezione di Milano, Milano, Italy

<sup>5</sup> Stefan-Meyer-Institut für Subatomare Physik, Vienna, Austria

<sup>6</sup> Excellence Cluster Universe, Technische Universität München Garching, Germany

<sup>7</sup> RIKEN, Tokyo, Japan

<sup>8</sup> Faculty of Physics, Astronomy, and Applied Computer Science, Jagiellonian University, Łojasiewicza 11, 30-348 Kraków, Poland

<sup>9</sup> Centro Ricerche Enrico Fermi—Museo Storico della Fisica e Centro Studi e Ricerche ‘Enrico Fermi’, Via Panisperna 89A 00184, Roma, Italy

E-mail: [francesco.sgaramella@lnf.infn.it](mailto:francesco.sgaramella@lnf.infn.it) and [alessandro.scordo@lnf.infn.it](mailto:alessandro.scordo@lnf.infn.it)

Received 25 January 2022, revised 23 February 2022

Accepted for publication 14 March 2022

Published 1 April 2022



CrossMark

## Abstract

The SIDDHARTINO experiment at the DAΦNE collider of INFN-LNF, the pilot run for the SIDDHARTA-2 experiment which aims to perform the measurement of kaonic deuterium transitions to the fundamental level, has successfully been concluded in July 2021. The paper reports the main results of this

\*This article is dedicated to the memory of a colleague and friend George Beer, with whom some of us shared the adventure of strangeness physics for many years.

\*\*Authors to whom any correspondence should be addressed.



Original content from this work may be used under the terms of the [Creative Commons Attribution 4.0 licence](https://creativecommons.org/licenses/by/4.0/). Any further distribution of this work must maintain attribution to the author(s) and the title of the work, journal citation and DOI.

run, including the optimization of various components of the apparatus, among which the degrader needed to maximize the fraction of kaons stopped inside the target, through measurements of kaonic helium transitions to the 2p level. The obtained shift and width values are  $\varepsilon_{2p} = E_{\text{exp}} - E_{\text{e.m}} = 0.2 \pm 2.5(\text{stat}) \pm 2.0(\text{syst})$  eV and  $\Gamma_{2p} = 8 \pm 10$  eV(stat), respectively. This new measurement of the shift, in particular, represents the most precise one for a gaseous target and is expected to contribute to a better understanding of the kaon–nuclei interaction at low energy. The results obtained in this pilot run, combined with the foreseen additional veto systems and projected for the total 48 SDD arrays of the SIDDHARTA-2 final setup, represent a solid starting point for the successful measurement of the kaonic deuterium  $2p \rightarrow 1s$  transition, main goal of the experiment.

Keywords: kaonic helium, silicon drift detectors, x-rays, kaon–nucleon interaction

(Some figures may appear in colour only in the online journal)

## Introduction

Light kaonic atoms spectroscopy is a unique tool for the investigation of the low-energy strangeness quantum chromodynamics. Precise measurements of the radiative x-ray transitions towards low- $n$  levels of these systems provide information on the kaon–nucleus interaction at threshold which, in typical scattering experiments, would require an extrapolation towards zero energy, making them method-dependent.

In this context, a special role is played by the lightest kaonic atoms, namely kaonic hydrogen, deuterium, and helium. From the first two, the isospin-dependent antikaon–nucleon scattering lengths can be obtained from the measurements of the strong interaction induced shifts and widths of the 1s levels. Additional information on the strong interaction with many-body systems can be retrieved from transitions to the 2p level of kaonic helium 3 and 4 [1].

The kaonic hydrogen 1s level strong interaction induced shift and width have been successfully measured by the SIDDHARTA experiment in 2009 [2].

For what regards the effect of the strong interaction on the 2p level of kaonic helium isotopes, the pool of experimental data is rich. The E570 experiment at KEK, in Japan, delivered in 2007 the first measurement of the  $K^4\text{He}(3d \rightarrow 2p)$  transition in liquid helium [3], which was followed by the first measurement with a gaseous target obtained by SIDDHARTA together with the first measurement ever of  $K^3\text{He}(3d \rightarrow 2p)$  [4, 5]. More recently, the E62 experiment at JPARC in 2018 measured x-rays from both kaonic helium 3 and 4 liquid targets [6].

The kaonic deuterium measurement is a very challenging one, due to the fact that the yield of the x-ray transitions to the 1s level is expected to be about one order of magnitude lower than that of kaonic hydrogen. This measurement will be performed for the first time by the SIDDHARTA-2 experiment, presently under installation at the DAΦNE collider [7–10], scheduled to take data in 2022–2023. Before the SIDDHARTA-2 kaonic deuterium measurement, a pilot run with a reduced setup, SIDDHARTINO, was performed in 2021 during the commissioning of the DAΦNE collider.

The aim of this run was twofold: on one side, the optimization of the run conditions, including the collider luminosity measurement, the trigger system, and the x-ray silicon drift detectors (SDDs) [11]; on the other side, the optimization of the degrader used by the experiment to maximize the fraction of kaons stopped inside the gaseous helium target.

This second step was performed by measuring kaonic helium-4 transitions on the 2p level, which has a much higher yield [12] than the kaonic deuterium expected one.

The pilot SIDDHARTINO run also allowed to obtain the most precise measurement of kaonic helium transitions in a gaseous target, which is reported in this paper together with all the optimizations which allowed to obtain this record.

In section 1, the experimental apparatus is described, while in section 2 the detector calibration procedure, the background suppression tools, and the kaon degrader optimization are reported. In section 3, the results for the shift and the width of the kaonic helium-4 2p level are presented, while in section 4 the conclusions can be found.

## 1. SIDDHARTINO at the DAΦNE collider

DAΦNE [7–10] is a world-class double ring  $e^+e^-$  collider operating at the center of mass energy of the  $\phi$ -resonance ( $m_\phi = 1.02 \text{ GeV}/c^2$ ). The back-to-back  $K^+K^-$  pairs, resulting from its almost at-rest decay with a  $\simeq 50\%$  branching ratio [13], are characterized by low momentum ( $\simeq 127 \text{ MeV}/c$ ) and low energy spread ( $\delta p/p \simeq 0.1\%$ ), making this machine an ideal environment to perform precision spectroscopy measurements of kaonic atoms.

In 2008 the collider underwent a major upgrade in order to implement a new collision scheme, called crab-waist [8]. The new approach to collisions provides several advantages: it reduces the beam-beam tune shift in the horizontal plane, shrinks the longitudinal size of the overlap between colliding bunches, thus allowing one to increase the vertical focusing at the interaction point (IP) and, moreover, it cancels almost completely the parasitic crossings. The SIDDHARTA-2 experiment [14] at DAΦNE aims to perform the first measurement ever of the x-ray transitions to the fundamental level of kaonic deuterium which, combined with the kaonic hydrogen one performed by SIDDHARTA [2], will be used to obtain the antikaon–nucleon isospin dependent scattering lengths [15, 16], fundamental quantities for a better understanding of the strong interaction theory in the strangeness sector. Before performing this challenging measurement, during the DAΦNE collider commissioning phase in 2021, a pilot run was performed with a reduced version of the setup, SIDDHARTINO, installed in the IP of the accelerator. The goal of this run was to assess and optimize the performances of the machine and the experimental apparatus via a measurement of the kaonic helium transitions to the 2p level, made possible by the much higher yields of these transitions compared to the kaonic deuterium ones.

The main components of the SIDDHARTINO setup are similar to those of the SIDDHARTA one; new dimensions and positions of the single elements have been chosen, after an optimization performed by means of a GEANT4 MonteCarlo simulation, with the goal of maximizing the measured signal of x-rays emitted from kaonic atoms [14]. A sketch of the SIDDHARTINO experimental apparatus is shown in figure 1.

A cylindrical vacuum chamber evacuated below  $10^{-5}$  mbar, is placed above the DAΦNE IP and contains the target cell. The closed-cycle helium refrigerator cooling system, shown in the upper part of figure 1, is used to cool the target cell down to 25 K. A system composed of two x-ray tubes is employed for the *in situ* calibration of the SDDs; these are used to measure the x-rays emitted from the radiative transitions of kaonic atoms. The calibration takes advantage of the excitation of the fluorescence lines of high purity Ti–Cu targets. Finally, the two lead walls in figure 1 represent the shielding structures used to shelter the apparatus from the particles, mostly minimum ionizing particles (MIPs), lost from the  $e^+e^-$  rings mainly by the Touschek effect.

In the lower part of figure 1 the kaon trigger (KT) and the luminometer systems, both based on pairs of scintillators read at both ends by photomultipliers, as well as the target cell, are

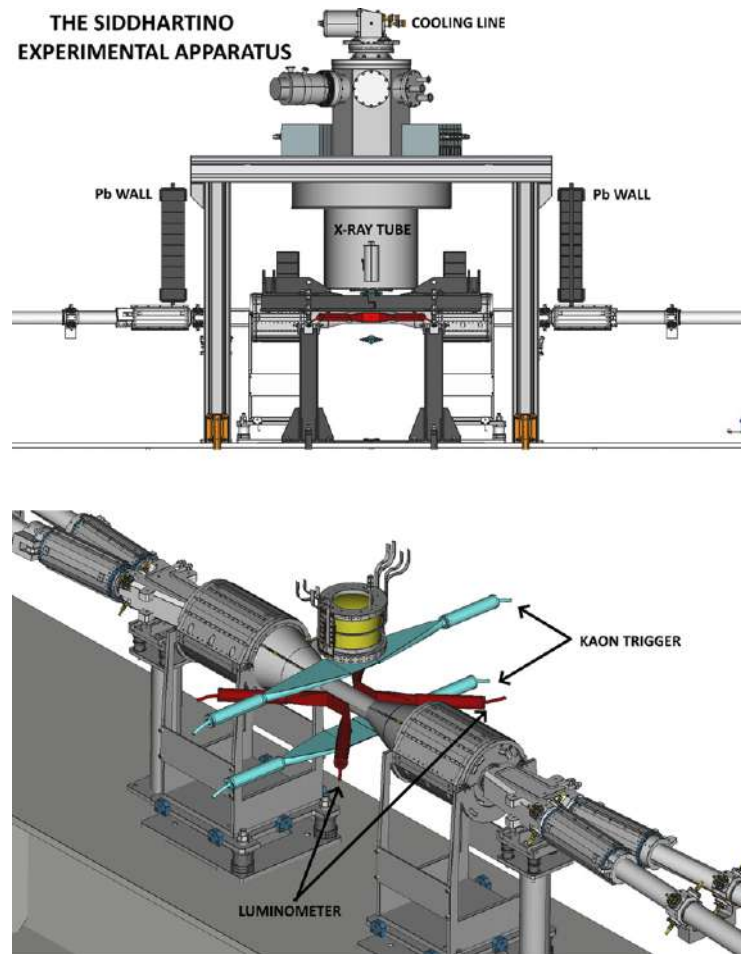


**Figure 1.** Top: schematic view of the SIDDHARTINO experimental apparatus installed on the IP of the DAΦNE collider. Bottom: view of the target cell, the kaon trigger (cyan), and the luminometer (red) systems.

shown. The luminometer, realized by the SIDDHARTINO-2 collaborators of the Jagiellonian University (red) is employed to evaluate both the machine luminosity and background via time of flight measurements of kaons and MIPs on the horizontal plane [17]. The  $K^+K^-$  pairs emitted from the  $\phi$  decay on the vertical plane are detected by the KT (cyan) before entering the target cell. The top scintillator is placed just in front of the entrance window of the vacuum chamber and it acts as an efficient asynchronous background rejection tool providing a narrow timing window to tag x-ray events in coincidence with kaons reaching the target.

The target cell is a cylinder of 144 mm in diameter and 125 mm in height, made of high purity aluminum bars and 150  $\mu\text{m}$  thick Kapton walls. It is placed inside the vacuum chamber above the beam pipe, it has a 125  $\mu\text{m}$  entrance window, a 100  $\mu\text{m}$  thick Ti top window and it is surrounded by 8 SDD arrays, with a dedicated thermal contact to keep them stable at the 170 K working temperature.

The large area monolithic SDD arrays have been developed by Fondazione Bruno Kessler (FBK, Trento), Politecnico di Milano (PoliMi), Laboratori Nazionali di Frascati (INFN-LNF), and the Stefan Meyer Institute (SMI, Vienna) specifically to be employed by the SIDDHARTA-2 experiment to perform high-precision spectroscopy of light kaonic atoms. Each 450  $\mu\text{m}$  thick silicon array consists of 8 single cells arranged in a  $2 \times 4$  matrix for a total active area of 5.12  $\text{cm}^2$ . The silicon wafer is glued on an alumina carrier which provides the polarization to the units via an external voltage. The charges generated by the x-ray absorption within the silicon bulk are collected by a point-like central anode and amplified through a closely bonded CMOS low-noise, charge-sensitive preamplifier. The signals are then processed by a dedicated ASIC which filters them through a 2  $\mu\text{s}$ , 9th order semi-Gaussian shaping stage to minimize the electronic noise contribution [18, 19]. Each ASIC handles the signals produced by 16 units and provides the data acquisition (DAQ) chain with the individual amplitude and timing information. The spectroscopic performances of this system have been optimized [20] and tested in the first DAΦNE commissioning phase where, with an energy resolution of  $157.8 \pm 0.3(\text{stat})_{-0.2}^{+0.2}(\text{syst})$  eV at 6.4 keV and a linearity at the level of 2–3eV [21], they proved to be suitable to perform high precision kaonic atoms measurements.

The second commissioning phase has been devoted to the fine tuning of the kaon degrader system (see section 2.3), one of the crucial components of the experiment. The purpose of the degrader is to slow down the kaons before entering the target cell to optimize their stopping distribution inside the gas target. For the optimization of the degrader, the SIDDHARTINO target cell has been filled with  $^4\text{He}$  gas at a temperature of 25 K and pressure of 1 bar, which corresponds to 1.5% of liquid helium density (LHeD). The high yield of the  $3d \rightarrow 2p$  transition of kaonic helium-4 ( $\text{K}^4\text{He}$ ) allowed to appreciate variations in the number of signal events at the level of  $\simeq 2\%$  in a few hours of data taking. The final period of the SIDDHARTINO data taking in June 2021 was dedicated to the measurement of  $\text{K}^4\text{He}(3d \rightarrow 2p)$  transitions at lower density, namely 0.4 bar, corresponding to 0.73% LHeD. In this work the results of the analysis performed on the summed spectra of 16.5  $\text{pb}^{-1}$  and 9.5  $\text{pb}^{-1}$  for the 1.5% and 0.73% LHeD runs, respectively, for a total integrated luminosity of 26  $\text{pb}^{-1}$  collected in about 20 days, are presented.

## 2. Data analysis and degrader optimization

### 2.1. Calibration procedure

The energy calibration of the SDDs is one of the most critical aspects of the whole data analysis procedure. It was performed using characteristic emission lines induced by the system of two x-ray tubes on high purity titanium and copper strips placed on the target cell walls. Since SDD cells and their associated front-end electronics are characterized by different charge collection and voltage conversion functions, individual calibrations are mandatory before summing up all the measured spectra [21]. Periodic calibration runs during the whole data taking period were thus performed to obtain the energy response of the single detectors. Figure 2 shows a typical spectrum for a single SDD obtained in a calibration run ( $\sim 1$  h). The peaks present in the spectrum, corresponding to the x-rays emitted by the activated titanium and copper strips, were fitted using a Gaussian plus an exponential low energy tail to reproduce the SDD response function [22]. The contribution of the low energy tail to the peak amplitude was found to be less than 1% [23]. Together with the calibration lines, other peaks are also visible (Mn, Fe, and Zn), resulting from the accidental excitation of various components of the experimental apparatus, which have been fitted with the same functions.

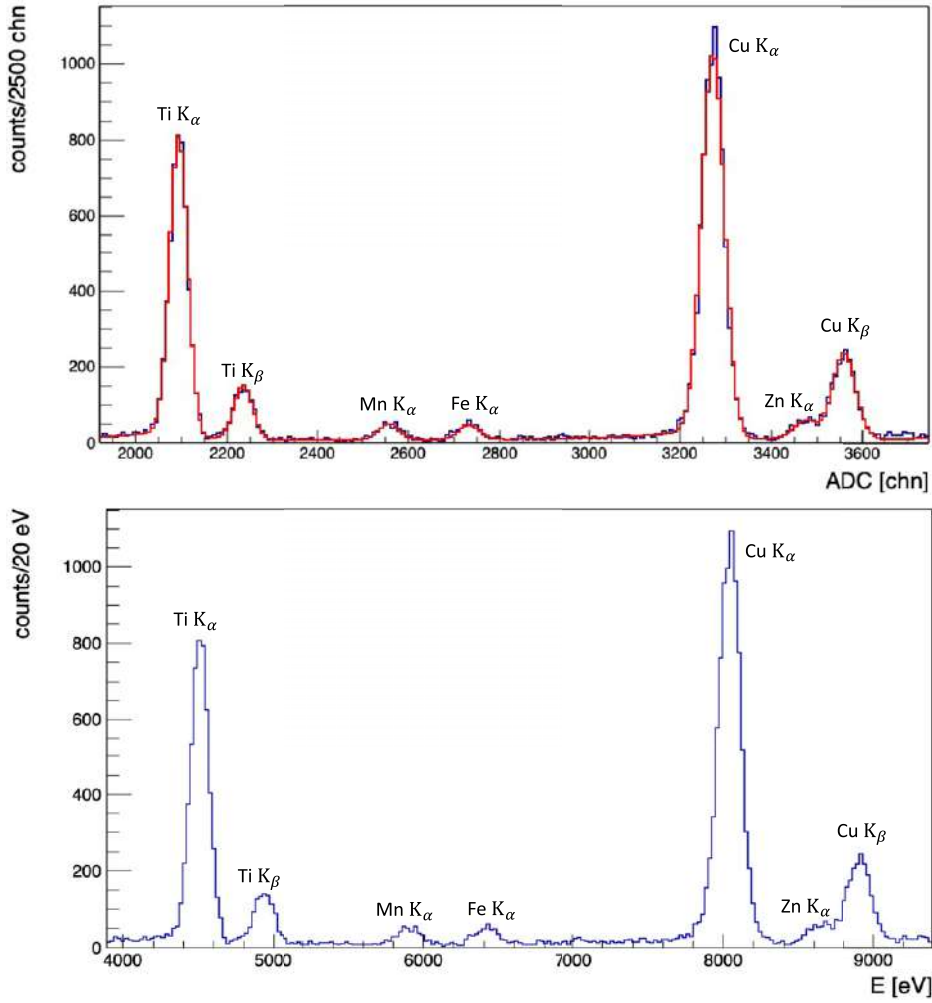


**Figure 2.** Top: typical spectrum for a single SDD obtained after a calibration run ( $\sim 1$  h of data taking); the calibration peaks (Ti and Cu) were fitted using a Gaussian function plus an exponential low energy tail. Mn, Fe and Zn come from the accidental excitation of various components of the experimental apparatus. The unit scale is given by the analog to digital converter (ADC). Bottom: typical calibrated spectrum for a single SDD.

The energy resolution of each SDD was evaluated from the Gaussian width ( $\sigma$ ), defined as function of the Fano factor (FF), the electron–hole pair energy creation ( $\epsilon$ ) and the electronic noise ( $n$ ):

$$\sigma = \sqrt{\text{FF} \cdot \epsilon \cdot E + \frac{n^2}{2.35^2}}. \quad (1)$$

The energy resolution obtained from the fit and extrapolated at the energy of the kaonic  $\text{K}^4\text{He } 3d \rightarrow 2p$  transition is  $157.0(\text{stat}) \pm 0.4(\text{syst})$  eV (FWHM), in agreement with the results already published [21].



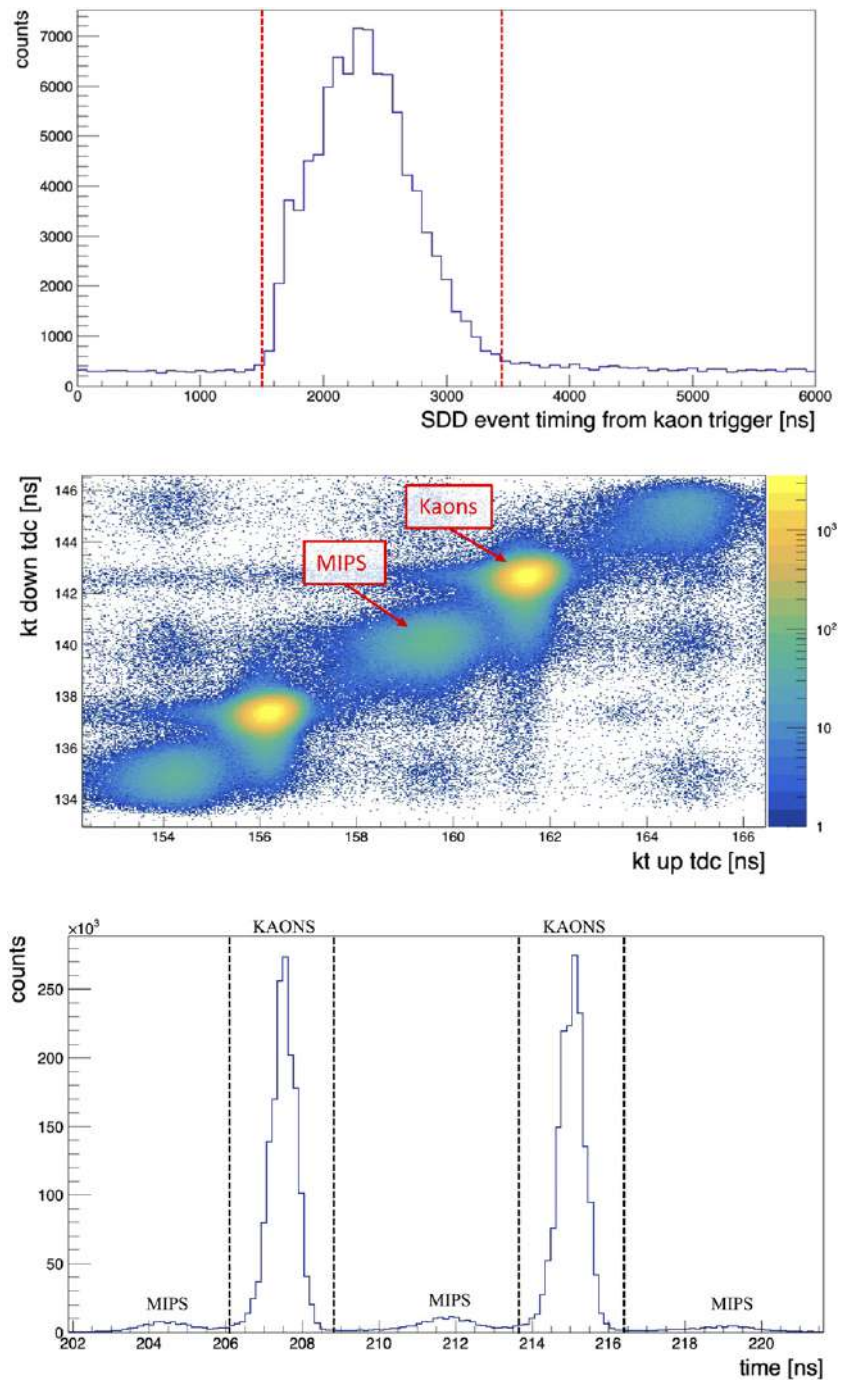


**Figure 3.** Time difference between a signal on the KT (up-down coincidence) and an SDD x-ray hit and the 1500 ns to 3450 ns acceptance window (top). Two-dimensional plot of the TDC for the upper and lower scintillators (mid) and its projection on the diagonal (bottom). The dotted lines represent the limits of the kaon selection time windows.



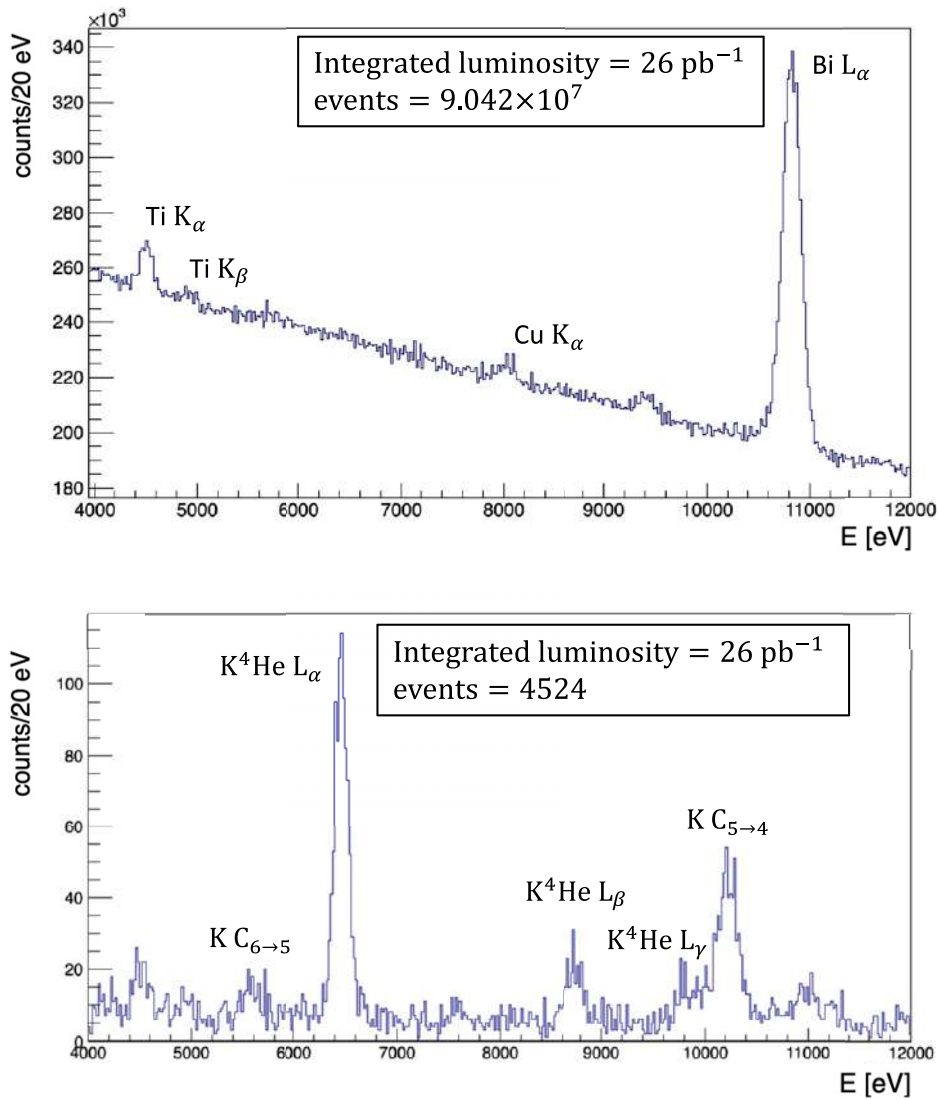


**Figure 4.** Spectra without (top) and with (bottom) KT selections, from which the  $\simeq 10^5$  rejection factor can be obtained (bottom). See text for details.

## 2.2. Background suppression

The background produced by the DAΦNE collider has two main components. The first one, mainly due to particles lost from the two rings (MIPs), is asynchronous with the  $e^+e^-$  collisions and can be highly suppressed using the KT; the second one, the synchronous background, corresponding to electromagnetic showers and heavier particles correlated in time with the collisions and the subsequent hadronic and electromagnetic processes, and is more difficult to suppress.

The additional VETO systems foreseen for the SIDDHARTA-2 experiment were not used in SIDDHARTINO because the main goal of this run was to assess and optimize the machine

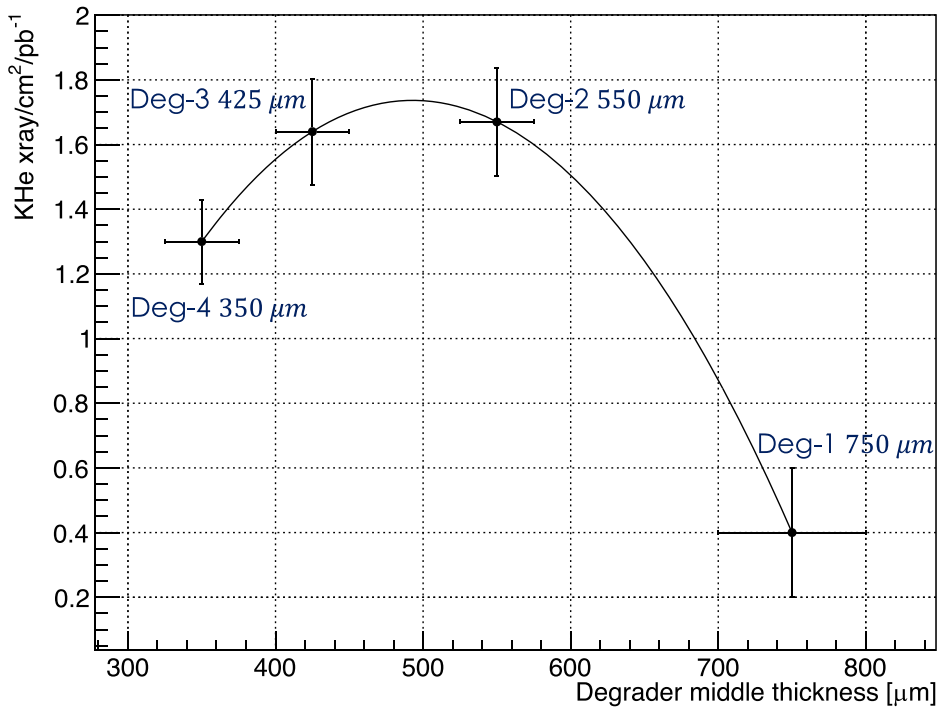


**Figure 5.** Degradation optimization curve: the horizontal axis is the central thickness and the vertical one the corresponding  $\text{K}^4\text{He}(3d \rightarrow 2p)$  signal normalized by integrated luminosity and effective detection surface.

conditions and compare them with the SIDDHARTA ones, where these systems were not present. Also, the risk, in unknown background conditions, to damage part of the detectors and of the various components led to the decision to use the SIDDHARTINO reduced version for the commissioning phase, while the complete VETO systems will be installed for the final SIDDHARTA-2 run.

The reduction of the asynchronous background is performed by selecting only the events occurring in time coincidence, within a  $5 \mu\text{s}$  window, with a signal on the KT. The time difference between the  $K^-K^+$  coincidence in the KT (up-down coincidence) and the time of the x-ray detection by SDDs is shown in the top part of figure 3, where the peak corresponds to x-ray signals on the SDDs in coincidence with the KT, while the flat distribution is the result of the uncorrelated events. The width of the peak is 950 ns (FWHM) and it reflects the drift time distribution of the electrons in the bulk of the SDDs. The region from 1500 ns to 3450 ns, delimited by the red dashed lines, is the drift time window selection. This trigger selection suppresses the background by a factor  $\simeq 10^5$ .

In addition to this selection, the time difference between the signals on each scintillator and the DAΦNE radiofrequency (RF) can be used to discriminate, via time of flight, whether an event on the KT is related to a kaon or to a MIP entering the target cell.

The middle pad of figure 3 shows the two-dimensional plot of the TDC for the upper and lower scintillators, while in the lower pad the projection on the diagonal is shown. The double KAONS/MIPs structure is due to the usage of the RF/2 signal as a time reference. From this figure, one can see the kaon-related events, corresponding to the two main peaks,

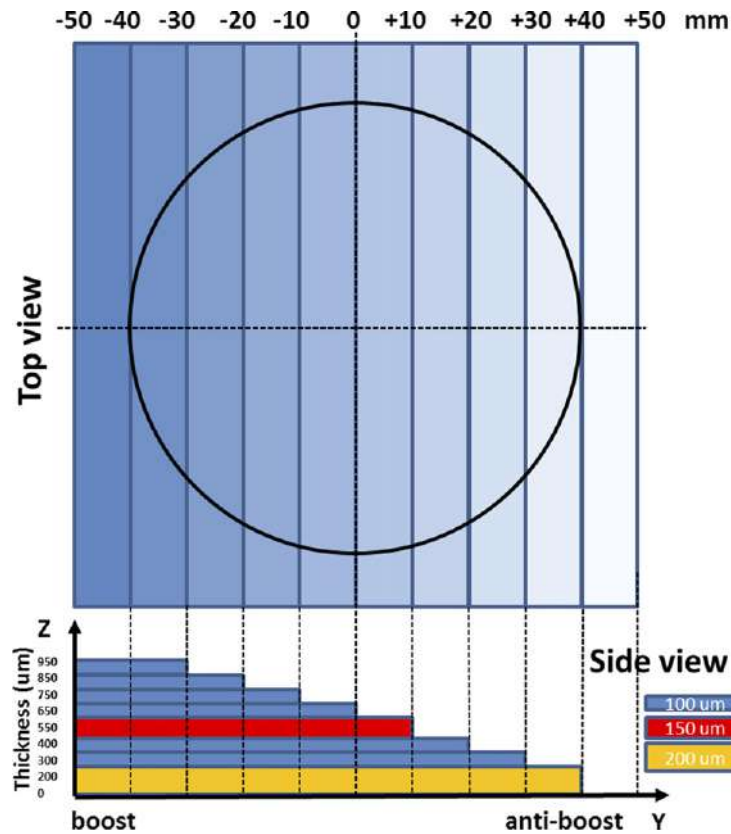


**Figure 6.** Nearest to optimal configuration of the Mylar degrader: the circle represents the size of the entrance window of the vacuum chamber; direction ‘Y’ points to the outer side of the DAΦNE ring, corresponding to the anti-boost side for kaons. The degrader has eight steps to compensate for the boost effect, with thicknesses shown in the lower part of the figure.

can be discriminated from the MIP-related ones. Among all triggered events only the kaon identified events, lying in the time windows within the dotted lines in figure 3, are finally accepted.

In the upper panel of figure 4, the inclusive kaonic helium-4 energy spectrum corresponding to  $26 \text{ pb}^{-1}$  integrated luminosity, with no background rejection, is shown. The continuous contribution below the peaks is mainly due to the asynchronous component of the machine background, while the Ti and Cu peaks originate from the calibration foils installed inside the target and activated by particles lost from the beams. The Bi peak was instead produced by the activation of the alumina carrier behind the SDDs silicon wafer. The region of interest for the  $\text{K}^4\text{He}(3d \rightarrow 2p)$  transition measurement lies around 6.4 keV. In this region no peaks potentially affecting the result of the measurement are present.

In the bottom panel of figure 4, the spectrum of the selected events is presented; here, the rejection capabilities of the KT can be appreciated; requiring the above mentioned triple coincidence and separating kaons and MIPs, a  $\simeq 10^5$  rejection factor is achieved and the  $\text{K}^4\text{He}(4d, 3d \rightarrow 2p)$  peaks are clearly observed.

### 2.3. Degradation optimization

Before entering the helium target, the kaons cross the beam pipe, the scintillators of the KT, the vacuum chamber, and target entrance windows; after passing through all these materials, the kaons need to be additionally slowed down to maximize the stopping fraction in the target. For this purpose, a degrader is placed below the upper scintillator of the KT, which has to be kept as close as possible to the entrance window of the target cell to reduce the probability of triggering kaons not reaching the gas target.

Since the trajectories of DAΦNE electron and positron beams cross, in the IP, at an angle of 50 mrad between each other, the center of mass of the subsequent  $K^+K^-$  system receives a boost towards the center of the collider, which is reflected in the momentum distribution of the kaons.

To compensate for this effect and to obtain a uniform stopping distribution of the kaons inside the target, a stepwise degrader is used. To optimize the shape and thickness of the degrader, MC simulations have been performed, as well as an experimental fine tuning, based on the amplitudes of the observed kaonic helium signals. For different degrader configurations, the number of  $K^4\text{He}(3d \rightarrow 2p)$  x-ray events, normalized to the integrated luminosity and effective detection surface was recorded and its trend as a function of the degrader central thickness is shown in figure 5. The degrader, which is schematically shown in figure 6 for the configuration nearest to the optimal one, consists of 8 Mylar strips of  $1 \times 9 \text{ cm}^2$  each varying from  $100 \mu\text{m}$  to  $200 \mu\text{m}$  thickness ( $550 \mu\text{m}$  in the central position, namely  $Y = 0$  in figure 6). The overall thickness of the eight-step degrader ranges from  $200 \mu\text{m}$  to  $950 \mu\text{m}$ .

This optimization is an important and delicate operation since, as clearly shown by the curve, even a small variation of about  $200 \mu\text{m}$  can drastically reduce the kaonic atoms signal.

### 3. The new $K^4\text{He}(3d \rightarrow 2p)$ shift and width measurement by SIDDHARTINO

Figure 7 shows the final  $K^4\text{He}$  spectrum for the total integrated luminosity of  $26 \text{ pb}^{-1}$ . The  $K^4\text{He} L\alpha$  line ( $3d \rightarrow 2p$ ) is visible together with the  $L\beta$  ( $4d \rightarrow 2p$ ) and  $L\gamma$  ( $5d \rightarrow 2p$ ) ones. Other lines, corresponding to kaonic carbon, nitrogen, and oxygen high- $n$  transitions generated by kaons stopped in the target window made of Kapton ( $\text{C}_{22}\text{H}_{10}\text{O}_5\text{N}_2$ ), were also detected, as well as lines from kaonic titanium and aluminum due to kaons stopping in the other components of the experimental apparatus.

The  $K^4\text{He}$  peaks were fitted with a Voigt function [4], the Gaussian part of which reproduces the detector energy response function, while the Lorentzian one describes the intrinsic linewidth of the transition. From the calibration procedure of the SDDs, it was found that the exponential low energy tails account for less than 1% of the peak amplitude, and hence are negligible for the kaonic helium peaks [23].

The other peaks were fitted using only the Gaussian part since the shift and broadening due to the strong interaction are known to be negligible for  $n > 2$  levels [3, 24]. The difference between the purely electromagnetic calculated transition energies and the experimental ones, representing the strong interaction induced shift, can be then set as a common parameter to all the  $K^4\text{He}$  peaks. Similarly to the shift parameter, also the strong interaction induced broadening of the  $2p$  level, representing the Lorentzian contribution to the Voigt function, can be set as a common parameter to all the  $K^4\text{He}$  lines. From the results of the fit the strong interaction induced shift and width of the  $2p$  level was measured to be:

$$\epsilon_{2p} = E_{\text{exp}} - E_{\text{e.m.}} = 0.2 \pm 2.5(\text{stat}) \pm 2.0(\text{syst}) \text{ eV} \quad (2)$$

$$\Gamma_{2p} = 8 \pm 10 \text{ eV (stat)}. \quad (3)$$

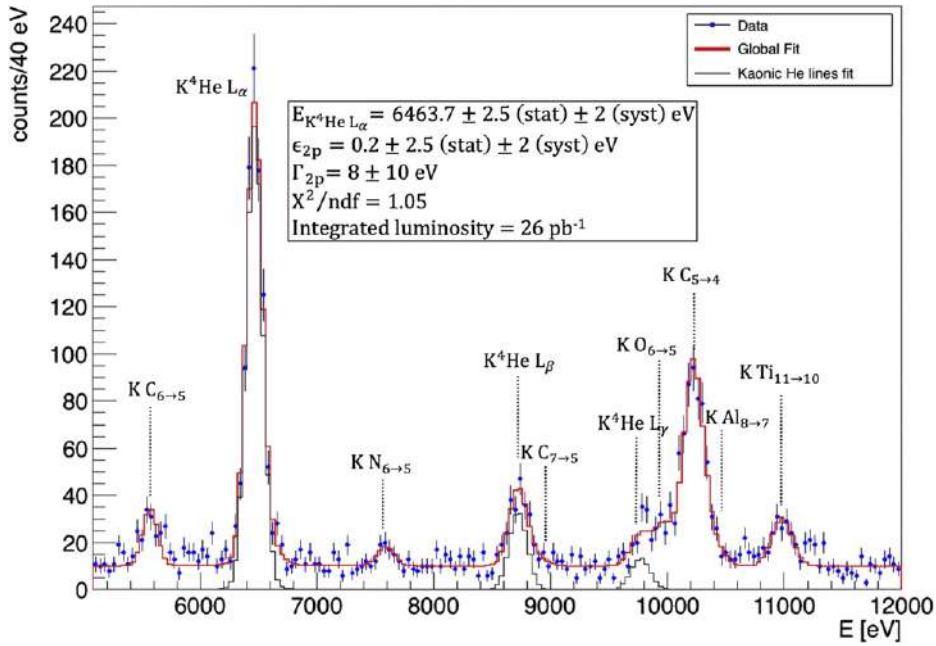


**Figure 7.** Fit (red line) of the  $K^4\text{He}$  energy spectrum. The  $L\alpha$  peak is seen together with the  $L\beta$  and  $L\gamma$  ones (black lines). The peaks labeled as KN, KC, KAl, KTi (dotted lines) are the kaonic atoms lines produced by the kaons stopped in the Kapton ( $\text{C}_{22}\text{H}_{10}\text{O}_5\text{N}_2$ ) walls of the target cell and in other parts of the setup (see text for details).

The systematic errors on the shift value were evaluated from the linearity and the stability of the energy response of the SDDs; other possible contributions (e.g. kaon timing window selection, different background contributions to the fit function) are negligible. The systematic errors on the width are negligible (less than 0.1 eV).

These results represent the most precise measurement of gaseous  $K^4\text{He}$  ( $3d \rightarrow 2p$ ) transition and confirm the experimental observations performed by the E570 [3] and the SIDDHARTA [4] experiments.

#### 4. Conclusions

The SIDDHARTINO experiment, the pilot run for the SIDDHARTA-2 experiment which aims to perform the first measurement ever for the kaonic deuterium transitions to the fundamental level, has successfully been concluded during the commissioning phase of the DAΦNE collider in the first half of 2021. During this run, a series of optimizations of the experimental apparatus, including that of the degrader, necessary for the optimization of the fraction of negatively charged kaons inside the cryogenic gaseous target, have been performed. The thin plastic degrader, shaped such as to take into account the boost of the  $\Phi$ -particles generating kaons with an energy-angle dependence, has been optimized at a precision level better than 100  $\mu\text{m}$ . The procedure exploited the kaonic helium-4 transitions to the 2p level measurements at an equivalent 1.5% liquid helium density. Also, a set of data at half of the previous density were collected.

The analysis of the overall set of kaonic helium data, for an integrated luminosity of 26  $\text{pb}^{-1}$ , has moreover delivered the most precise measurement of kaonic helium-4 x-ray

transitions in gas, in terms of shift and width of the 2p level induced by the strong interaction. The SIDDHARTINO results put an even more stringent limit than the previous SIDDHARTA outcome [4], and exclude large shifts and widths. Such results, on one side, contribute to a better understanding of the strong interaction at low-energy in systems with strangeness, even if more precise results are mandatory. On the other side, the successful completion of the SIDDHARTINO run proved the innovative technologies and methodologies employed by the collaboration in studies of exotic atoms in a collider environment are sound and solid. It sets the ground for the kaonic deuterium measurement with the SIDDHARTA-2 experiment, which has been fully installed on the DAΦNE collider at the beginning of 2022, aiming to perform its DAQ campaign from spring 2022 for an overall integrated luminosity of  $800 \text{ pb}^{-1}$ . This experiment will provide a kaonic deuterium measurement of the same level of precision as the kaonic hydrogen one performed by SIDDHARTA [2].

Other types of kaonic atom measurements with various radiation detectors are presently under consideration, to be proposed and performed after the SIDDHARTA-2 run. They could further contribute to a deeper understanding of the strong interaction in the low-energy regime in the strangeness sector, impacting particle and nuclear physics and also astrophysics [25].

## Acknowledgments

We thank C Capocchia from LNF-INFN and H Schneider, L Stohwasser, and D Pristauz-Telsnigg from Stefan-Meyer-Institut for their fundamental contribution in designing and building the SIDDHARTA-2 setup. We thank as well the DAΦNE staff for the excellent working conditions and permanent support. Part of this work was supported by the Austrian Science Fund (FWF): [P24756-N20 and P33037-N]; the Croatian Science Foundation under the project IP-2018-01-8570; EU STRONG-2020 project (Grant Agreement No. 824093), the EU Horizon 2020 project under the MSCA GA 754496 and the Polish Ministry of Science and Higher Education Grant No. 7150/E-338/M/2018 and the Foundational Questions Institute and Fetzer Franklin Fund, a donor-advised fund of Silicon Valley Community Foundation (Grant No. FQXi-RFP-CPW-2008).

## Data availability statement

The data that support the findings of this study are available upon reasonable request from the authors.

## ORCID iDs

F Sgaramella  <https://orcid.org/0000-0002-0011-8864>  
D Bosnar  <https://orcid.org/0000-0003-4784-393X>  
R Del Grande  <https://orcid.org/0000-0002-7599-2716>  
M Miliucci  <https://orcid.org/0000-0002-2315-2379>  
P Moskal  <https://orcid.org/0000-0002-4229-3548>  
F Napolitano  <https://orcid.org/0000-0002-8686-5923>  
A Scordo  <https://orcid.org/0000-0002-7703-7050>



## References

- [1] Curceanu C *et al* 2019 *Rev. Mod. Phys.* **91** 025006
- [2] Bazzi M *et al* 2011 *Phys. Lett. B* **704** 113
- [3] Okada S *et al* 2007 *Phys. Lett. B* **653** 387–91
- [4] Bazzi M *et al* (SIDDHARTA) 2012 *Phys. Lett. B* **714** 40–3
- [5] Bazzi M *et al* (SIDDHARTA) 2011 *Phys. Lett. B* **697** 199–202
- [6] De Paoli s L 2021 *PhD Thesis*
- [7] Vignola G *et al* 1996 *Conf. Proc. C* **960610** 22–6
- [8] Raimondi P, Shatilov D N and Zobov M 2007 Beam-beam issues for colliding schemes with large PIWINSKI angle and crabbed waist (arXiv:[physics/0702033](https://arxiv.org/abs/physics/0702033))
- [9] Zobov M *et al* 2010 *Phys. Rev. Lett.* **104** 174801
- [10] Milardi C *et al* 2018 Preparation activity for the Siddharta-2 run at DAΦNE *9th Int. Particle Accelerator Conference, IPAC2018* (Vancouver BC Canada)
- [11] Miliucci M *et al* 2021 *Condens. Mat.* **6** 47
- [12] Bazzi M *et al* 2014 *Eur. Phys. J. A* **50** 91
- [13] Zyla P *et al* (Particle Data Group) 2020 *PTEP* **2020** 083C01
- [14] SIDDHARTA-2 Collaboration 2010 *SIDDHARTA-2 Proposal, LNF Internal Notes* ([https://lnf.infn.it/committee/private/documenti/SIDDHARTA2-proposal\\_FINAL.pdf](https://lnf.infn.it/committee/private/documenti/SIDDHARTA2-proposal_FINAL.pdf))
- [15] Döring M and Meißner U G 2011 *Phys. Lett. B* **704** 663
- [16] Shevchenko N 2017 *Nucl. Phys. A* **890–891** 50
- [17] Skurzok M *et al* 2020 *JINST* **15** P10010
- [18] Quaglia R *et al* 2016 *Nucl. Instrum. Methods Phys. Res. A* **824** 449–51
- [19] Schembari F, Quaglia R, Bellotti G and Fiorini C 2016 *IEEE Trans. Nucl. Sci.* **63** 1797
- [20] Miliucci M, Iliescu M, Amirkhani A, Bazzi M, Curceanu C, Fiorini C, Scordo A, Sirghi F and Zmeskal J 2019 *Condens. Matter.* **4** 31
- [21] Miliucci M *et al* 2021 *Meas. Sci. Technol.* **32** 095501
- [22] Van Gysel M, Lemberge P and Van Espen P 2003 *X-Ray Spectrom.* **32** 434–41
- [23] SIDDHARTA-2 Collaboration 2021 *J. Phys. D: Appl. Phys.* submitted
- [24] Friedman E, Gal A and Batty C J 1994 *Nucl. Phys. A* **579** 518–38
- [25] Curceanu C *et al* 2021 *Few Body Syst.* **62** 83